

RESEARCH PAPER



## A functional genomic approach to identify reference genes for human pancreatic beta cell real-time quantitative RT-PCR analysis

Maria Inês Alvelos<sup>a\*</sup>, Florian Szymczak<sup>a\*</sup>, Ângela Castela<sup>a</sup>, Sandra Marín-Cañas<sup>a</sup>, Bianca Marmontel de Souza<sup>a</sup>, Ioannis Gkantounas<sup>a</sup>, Maikel Colli<sup>a</sup>, Federica Fantuzzi<sup>a</sup>, Cristina Cosentino<sup>a</sup>, Mariana Igoillo-Esteve<sup>a</sup>, Lorella Marselli<sup>b</sup>, Piero Marchetti<sup>b</sup>, Miriam Cnop<sup>a,c</sup>, and Décio L. Eizirik<sup>a,d,e</sup>

<sup>a</sup>ULB Center for Diabetes Research, Medical Faculty, Université Libre De Bruxelles, Brussels (ULB) Belgium; <sup>b</sup>Department of Clinical and Experimental Medicine, Islet Cell Laboratory, University of Pisa, Pisa, Italy; <sup>c</sup>Division of Endocrinology, Erasmus Hospital, Université Libre De Bruxelles, Brussels, Belgium; <sup>d</sup>Welbio, Medical Faculty, Université Libre De Bruxelles, Brussels (ULB) Belgium; <sup>e</sup>Diabetes Center, Indiana Biosciences Research Institute, Indianapolis, IN, USA

### ABSTRACT

Exposure of human pancreatic beta cells to pro-inflammatory cytokines or metabolic stressors is used to model events related to type 1 and type 2 diabetes, respectively. Quantitative real-time PCR is commonly used to quantify changes in gene expression. The selection of the most adequate reference gene(s) for gene expression normalization is an important pre-requisite to obtain accurate and reliable results. There are no universally applicable reference genes, and the human beta cell expression of commonly used reference genes can be altered by different stressors. Here we aimed to identify the most stably expressed genes in human beta cells to normalize quantitative real-time PCR gene expression.

We used comprehensive RNA-sequencing data from the human pancreatic beta cell line EndoC-βH1, human islets exposed to cytokines or the free fatty acid palmitate in order to identify the most stably expressed genes. Genes were filtered based on their level of significance (adjusted *P*-value >0.05), fold-change (|fold-change| <1.5) and a coefficient of variation <10%. Candidate reference genes were validated by quantitative real-time PCR in independent samples.

We identified a total of 264 genes stably expressed in EndoC-βH1 cells and human islets following cytokines – or palmitate-induced stress, displaying a low coefficient of variation. Validation by quantitative real-time PCR of the top five genes *ARF1*, *CWC15*, *RAB7A*, *SIAH1* and *VAPA* corroborated their expression stability under most of the tested conditions. Further validation in independent samples indicated that the geometric mean of *ACTB* and *VAPA* expression can be used as a reliable normalizing factor in human beta cells.

### ARTICLE HISTORY

Received 14 April 2021  
Revised 22 June 2021  
Accepted 22 June 2021

### KEYWORDS



Reference genes/ beta cells/  
diabetes/ RNA-sequencing/  
quantitative real-time pcr

## Introduction

The study of molecular mechanisms involved in pancreatic beta cell dysfunction and death in type 1 (T1D) and type 2 diabetes (T2D) often involves *in vitro* exposure of human beta cells to stressors that may be present *in vivo* in T1D and T2D.<sup>1–3</sup> Exposure of beta cells to these stressors, including pro-inflammatory cytokines (as a model of T1D) or palmitate (as a model of metabolic stress in T2D), substantially alters their gene expression.<sup>2,4</sup>

Quantitative real-time polymerase chain reaction (qPCR) is a commonly used technique to measure mRNA transcript levels owing to its sensitivity, specificity and fast execution.<sup>5</sup> The accurate quantification of the observed changes relies on the effective

normalization to one or more reference gene(s), whose expression should not be altered by the experimental condition(s) under evaluation. A unique and universal reference gene has not yet been identified, and therefore gene expression normalization usually depends on genes classified as “housekeeping genes” which, due to their cellular indispensability, are assumed to have stable expression under different experimental conditions. Commonly used reference genes, such as *beta actin (ACTB)*, *beta-2-microglobulin (B2M)*, the *18 S ribosome small subunit (18S rRNA)* and *glyceraldehyde-3-phosphate dehydrogenase (GAPDH)*, are widely used as normalizers due to their robust expression.<sup>6,7</sup> However, their expression varies widely among conditions and cell types,<sup>8–11</sup>

**CONTACT** Maria Inês Alvelos  [mardeoli@ulb.ac.be](mailto:mardeoli@ulb.ac.be)  ULB Center for Diabetic Research, Medical Faculty, Université Libre De Bruxelles (ULB), Route De Lennik, 808 – CP618, B-1070 – Brussels – Belgium

\*The first two authors should be regarded as joint First Authors.

© 2021 The Author(s). Published with license by Taylor & Francis Group, LLC.

This is an Open Access article distributed under the terms of the Creative Commons Attribution-NonCommercial-NoDerivatives License (<http://creativecommons.org/licenses/by-nc-nd/4.0/>), which permits non-commercial re-use, distribution, and reproduction in any medium, provided the original work is properly cited, and is not altered, transformed, or built upon in any way.

including pancreatic islets.<sup>12,13</sup> An inadequate selection of reference genes – that are up – or down-regulated in parallel with the gene under study – could lead to the misinterpretation of qPCR results and obscure genuine changes.

There are few studies on the identification of reference genes in human beta cells, and they are mostly limited to show that the housekeeping gene does not change under the experimental conditions used.<sup>14</sup> Rat islets of Langerhans have different expression levels of reference genes during the first 24 hours following isolation,<sup>13</sup> and a study in rat insulin-secreting INS-1E cells confirmed that qPCR results are affected by the normalization method and selected reference genes.<sup>15</sup>

Selection of the most suitable reference genes should be implemented through the validation of their expression stability in the cell or tissue type under the study. Most studies use bioinformatic tools such as BestKeeper,<sup>16</sup> geNorm,<sup>17</sup> NormFinder,<sup>18</sup> or Global Pattern Recognition,<sup>19</sup> which perform a mathematical evaluation of gene expression and rank candidates according to their stability. These tools define the least variable genes from a list of pre-selected candidate genes, but they are not suitable for *de novo* identification of genes with calibrating potential.

Against this background, a genome-wide analysis to identify stable and well-expressed genes in human islets and beta cells represents an essential tool for accurate normalization. To achieve this goal, we used high-depth RNA-sequencing data from the human beta cell line EndoC- $\beta$ H1 and human islets exposed to pro-inflammatory cytokines or palmitate. Genes were validated as putative reference genes by qPCR in EndoC- $\beta$ H1 cells, human islets and induced pluripotent stem cell (iPSC)-derived islets.

## Results

### *In silico* selection of new reference genes

The analysis of high-depth RNA-seq (around 200 million reads) data from insulin-producing EndoC- $\beta$ H1 cells exposed to the pro-inflammatory cytokines interleukin-1 $\beta$  (IL1 $\beta$ ) plus interferon- $\gamma$  (IL1 $\beta$  + IFN $\gamma$ ) for 48 h, or interferon- $\alpha$  (IFN $\alpha$ ) for 2 h, 8 h, and 24 h and human islets exposed to IL1 $\beta$  + IFN $\gamma$  for 48 h or IFN $\alpha$  for 2 h, 8 h, and 18 h, or the

metabolic stressor palmitate for 48 h (Figure 1A) (see references in Methods) indicated that  $17,874 \pm 3,751$  genes are not significantly modified, according to the criteria of an adjusted *P*-value  $>0.05$  and  $|\text{fold-change}| <1.5$ . The gene expression level quantified as transcripts per million (TPM) was used to evaluate intra – and inter-experimental condition expression variability. A total of 264 genes displays a coefficient of variation (CV)  $<10\%$ , of which 175 genes have a mean TPM between 10 and 100, and 89 a mean TPM between 100 and 1000 (Figure 1B–D) (Supplementary Table 1). Genes with mean TPM  $>1000$  (Figure 1B, C, D) have the highest mean CV. For this reason, we selected the candidate reference genes among the low ( $10 < \text{mean TPM} < 100$ ) and intermediate TPM ( $100 < \text{mean TPM} < 1000$ ) intervals. Gene Ontology (GO) enrichment analysis on this set of 264 genes revealed an enrichment in pathways associated with central cellular functions such as “intracellular transport,” “mRNA processing,” “RNA splicing,” and “protein catabolic processes” (adjusted *P*-value  $<0.05$ ) (Figure 1E). As a proof of concept, we selected five genes: *ADP-ribosylation factor 1* (*ARF1*), *spliceosome associated protein homolog* (*CWC15*), *member RAS oncogene family* (*RAB7A*), *E3 ubiquitin protein ligase 1* (*SIAH1*) and *vesicle-associated membrane protein-associated protein A* (*VAPA*) from the 264 candidates for subsequent validation. Except for *RAB7A*,<sup>21</sup> none of the genes have been previously used as reference genes in human beta cells or other tissues. The mean CV for the selected 5 genes ranged from 7% to 8.4%, and they were more stably expressed in human beta cells as compared to *ACTB* and *GAPDH*, which have CVs of 17.9% and 23.4%, respectively (Figure 1C, D). Interestingly, *ARF1*, *CWC15*, *RAB7A*, *SIAH1*, *VAPA* genes have the same mean TPM distribution and CV in beta cells from T1D and T2D donors and their respective non-diabetic controls, reinforcing our observation that these genes are stably expressed, and may be suitable human beta cell reference genes (Supplementary Figure 1A, B).

### Validation of gene expression stability by quantitative real time PCR (qPCR)

In order to assess the validity of the RNA-seq findings, we quantified by qPCR the expression of the

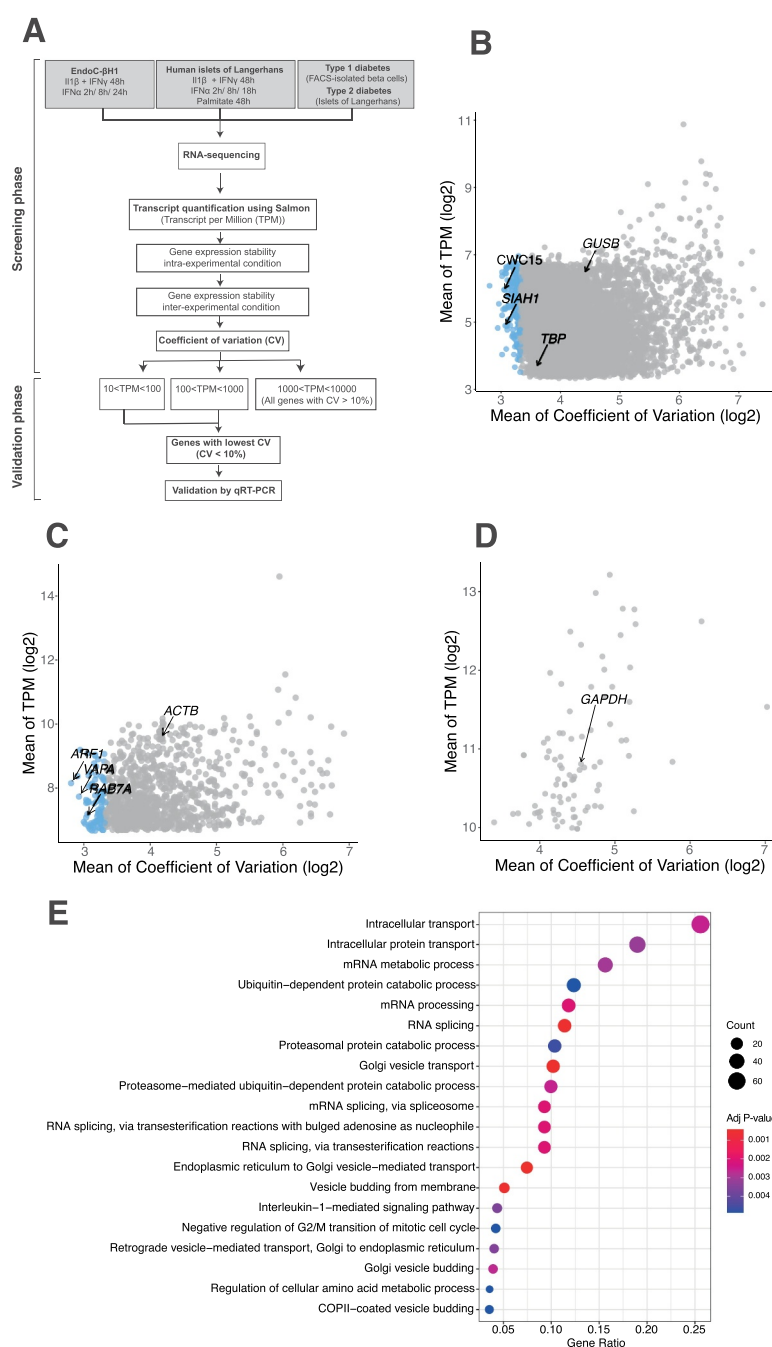


**Figure 1. Identification of new reference genes for human islets/beta cells. (A)** The approach for the identification of new reference genes in human pancreatic beta cells started with the analysis of RNA-sequencing data from EndoC-βH1 cells exposed to IL1β + IFNγ (48 h, n = 5) or IFNα (2 h, 8 h, and 24 h, n = 5 per time point); human islets exposed to IL1β + IFNγ (48 h, n = 5) or IFNα (2 h, 8 h, and 18 h, n = 6 per time point); human islets exposed to palmitate (48 h, n = 5); fluorescence-activated cell sorting (FACS)-purified beta cells from T1D patients (n = 4), and islets from T2D patients (n = 28). The quantification of expression of gene transcripts was conducted using Salmon v1.3.0 (Genome reference: GENCODE GRCh38.p13).<sup>20</sup> Transcript expression levels, measured in transcripts per million (TPM), were used to calculate the intra- and inter-sample stability, and their respective coefficient of variation (CV). TPM values were subdivided in three categories: 10 < TPM < 100; 100 < TPM < 1000; 1000 < TPM < 10,000. Genes with the lowest mean CV were selected for further validation by qRT-PCR. **(B,C,D)** Scatterplots of mean CV against mean expression values (TPM) after log<sub>2</sub> transformation based on RNA-seq data, for genes with TPM values between 10 and 100 **(B)**, between 100 and 1000 **(C)**, and between 1000 and 10,000 **(D)**. Each circle represents a gene with an adjusted *P*-value > 0.05, |fold-change| < 1.5, and blue circles represent the genes with CV < 10%. Selected reference genes are shown in the scatterplots, along with the well-established reference genes *ACTB* and *GAPDH*. **(E)** Significantly enriched Gene Ontology (GO) terms by gene enrichment analysis of the 264 genes with adjusted *P*-value > 0.05, |foldchange| < 1.5 and CV < 10%. The gene ratio represents the ratio between the genes in the GO term that overlaps with the query gene list (the short list of candidate genes with CV < 10%). The top 20 enriched GO terms are represented. Adjusted *P*-value from hypergeometric distribution (Benjamini-Hochberg).

**Table 1.** Information about the different cell types and treatment conditions used in the present study.

Cell type	Treatment	Incubation time (hours)	Concentration (units)	Number of samples analyzed per gene
EndoC-βH1	IL1β + IFNγ	48 h	50 U/mL + 1,000 U/mL	6 – 12
EndoC-βH1	IL1β + IFNα	48 h	50 U/mL + 2000 U/mL	6–13
EndoC-βH1	IFNα	8 h	2000 U/mL	6
EndoC-βH1	IFNα	24 h	2000 U/mL	12–13
EndoC-βH1	Thapsigargin	24 h	1 μM	3–9
EndoC-βH1	Tunicamycin	48 h	5 μg/mL	6
Human islets	IL1β + IFNγ	48 h	50 U/mL + 1,000 U/mL	4
Human islets	Palmitate	48 h	0.5 mmol/L	4
Human islets	IFNα	8 h	2000 U/mL	4
Human islets	IFNα	24 h	2000 U/mL	4
iPSCs-beta cells (WS)	IFNα	24 h	2000 U/mL	4
iPSCs-beta cells (WS)	IL1β + IFNγ	24 h	50 U/mL + 1,000 U/mL	4
iPSCs-beta cells (WS)	IFNα	48 h	2000 U/mL	4
iPSCs-beta cells (WS)	IL1β + IFNγ	48 h	50 U/mL + 1,000 U/mL	4
iPSCs-beta cells	Palmitate	24 h	0.5 mmol/L	4

IL1β, Interleukin 1β; IFNγ, Interferon γ; IFNα, Interferon α; iPSCs, induced pluripotent stem cells; WS, Wolfram syndrome.

five selected potential reference genes (*ARF1*, *CWC15*, *RAB7A*, *SIAH1*, *VAPA*) and the commonly used (*ACTB* and *GAPDH*) reference genes in independent samples of EndoC-βH1 cells and human islets exposed to different stress conditions. To allow accurate comparison between samples, all of them were diluted to the same final cDNA concentration, as described in Methods. PCR amplification efficiency was >90% for all genes.

The exposure of EndoC-βH1 cells to IL1β + IFNγ or IL1β + IFNα did not modify the expression of the analyzed reference genes (Figure 2A, B). However, IFNα modified expression of several of them, including *GAPDH* and *ACTB* (Figure 2C, D), which might be related to the induction of an acute anti-viral response by IFNα that modifies chromatin opening and the expression of thousands of genes.<sup>22</sup> Although *ACTB* and *GAPDH* have higher CV values compared to the novel reference genes in the RNA-seq data (Figure 1C and D), qPCR of these genes indicated stable expression in most conditions (Figures 2, 3, 4, Supplementary Figure 1) except for IFNα exposure. A combination of reference genes can provide more accurate correction for mRNA loading.<sup>26</sup> We selected *ACTB* and *VAPA* because they are amongst the most well-expressed genes, displaying quantification cycle (Cq) values between 17–28 and 20–28, respectively, and they also do not change following exposure to different stresses (Figure 1). Additionally, at least for *ACTB*, this gene is already in use by many islet research laboratories. We calculated the geometric mean between *ACTB* and

*VAPA* Cq values and included them for comparison in the figures.

We next tested the effect of thapsigargin (TG) and tunicamycin (TM), two commonly used chemical endoplasmic reticulum stressors. EndoC-βH1 cells exposed to TG for 24 h or TM for 48 h neither showed differences in Cq values of the five new reference genes nor on *ACTB* and *GAPDH* expression (Supplementary Figure 1C, D).

Due to the limited amount of human islet material available, we restricted our analysis to *ACTB* and *VAPA*. IL1β + IFNγ, IFNα or palmitate did not change expression of *ACTB* and *VAPA* genes in human islets (Figure 3). Using available single cell RNA-sequencing data from the Human Islet Analysis Program (HPAP),<sup>27</sup> we confirmed that both *ACTB* and *VAPA* are expressed in all endocrine and non-endocrine cells from isolated human islets from non-diabetic and T1D donors (Supplementary Figure 2A–D). The expression of *VAPA* was less variable as compared with *ACTB* among the different cell types (Supplementary Figure 2C, D). iPSC-derived beta cells represent a new model to study pathophysiologic mechanisms in T1D and T2D.<sup>24,28–32</sup> We analyzed candidate reference genes in iPSC-derived islets exposed to the pro-inflammatory cytokines IFNα, IL1β + IFNγ and palmitate (Figure 4A, B, C). None of these stressors altered the expression of the genes, suggesting that they are suitable for qPCR data normalization in iPSC-derived islets.

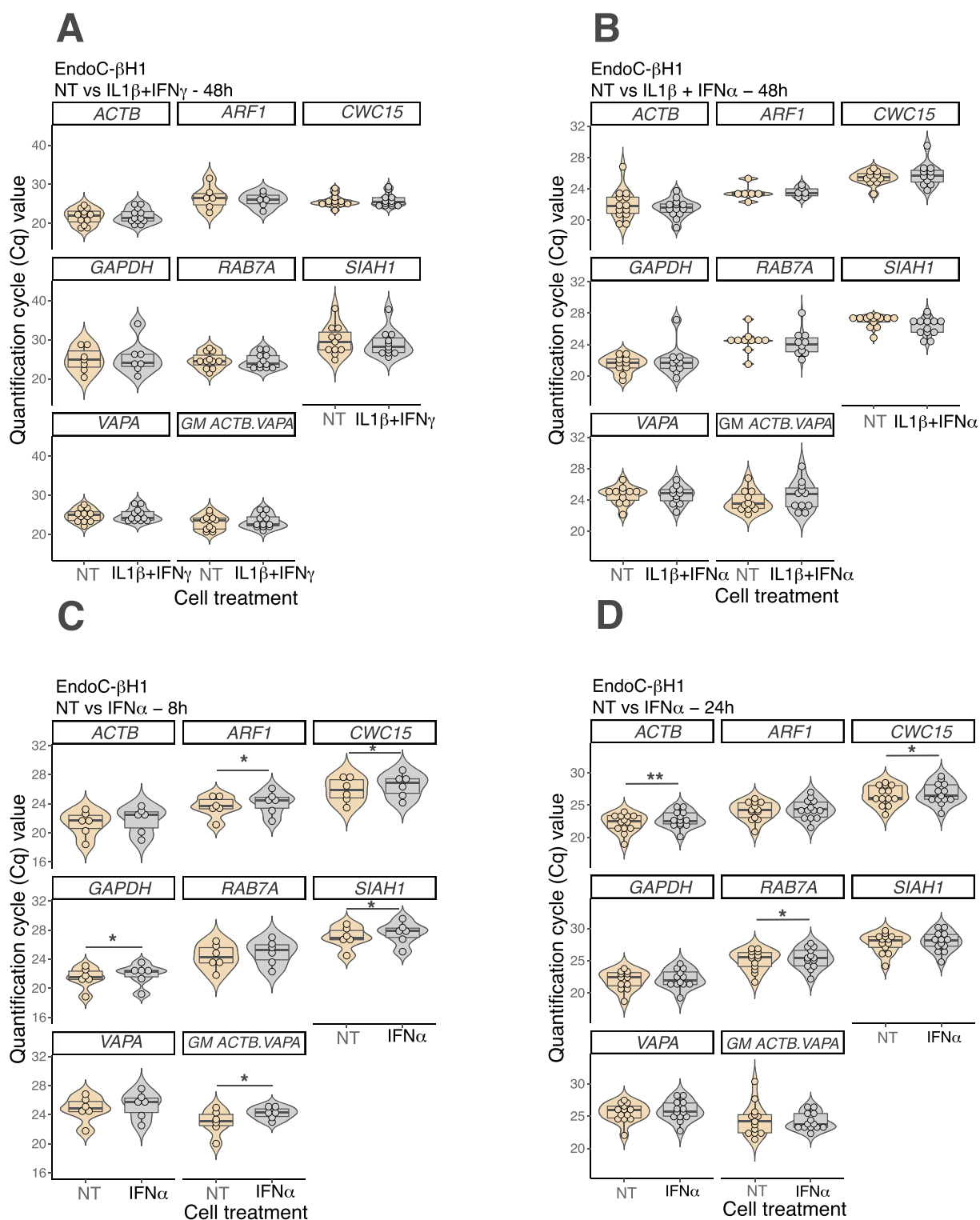


**Figure 2. Validation of reference genes by qPCR in EndoC- $\beta$ H1 cells.** Distribution of the quantification cycle (Cq) value of five new (*ARF1*, *CWC15*, *RAB7A*, *SIAH1*, *VAPA*) and two commonly used reference genes (*ACTB* and *GAPDH*) based on qPCR, in EndoC- $\beta$ H1 cells treated with IL1 $\beta$  + IFN $\gamma$  for 48 h (**A**), IL1 $\beta$  + IFN $\alpha$  for 48 h (**B**), IFN $\alpha$  for 8 h (**C**) and 24 h (**D**). Geometric means of *ACTB* and *VAPA* Cq values were also calculated (*GM ACTB.VAPA*). The shape of the violin plots reflects the distribution of the data, and the width of curve corresponds to the frequency of values in each region. The boxplots show the 25<sup>th</sup> and 75<sup>th</sup> percentiles, and the horizontal line represents the median. Each data point represents one qPCR replicate from six to thirteen independent experiments. \*P < .05, \*\*P < .01 versus not-treated (NT) (paired Student's t-test).

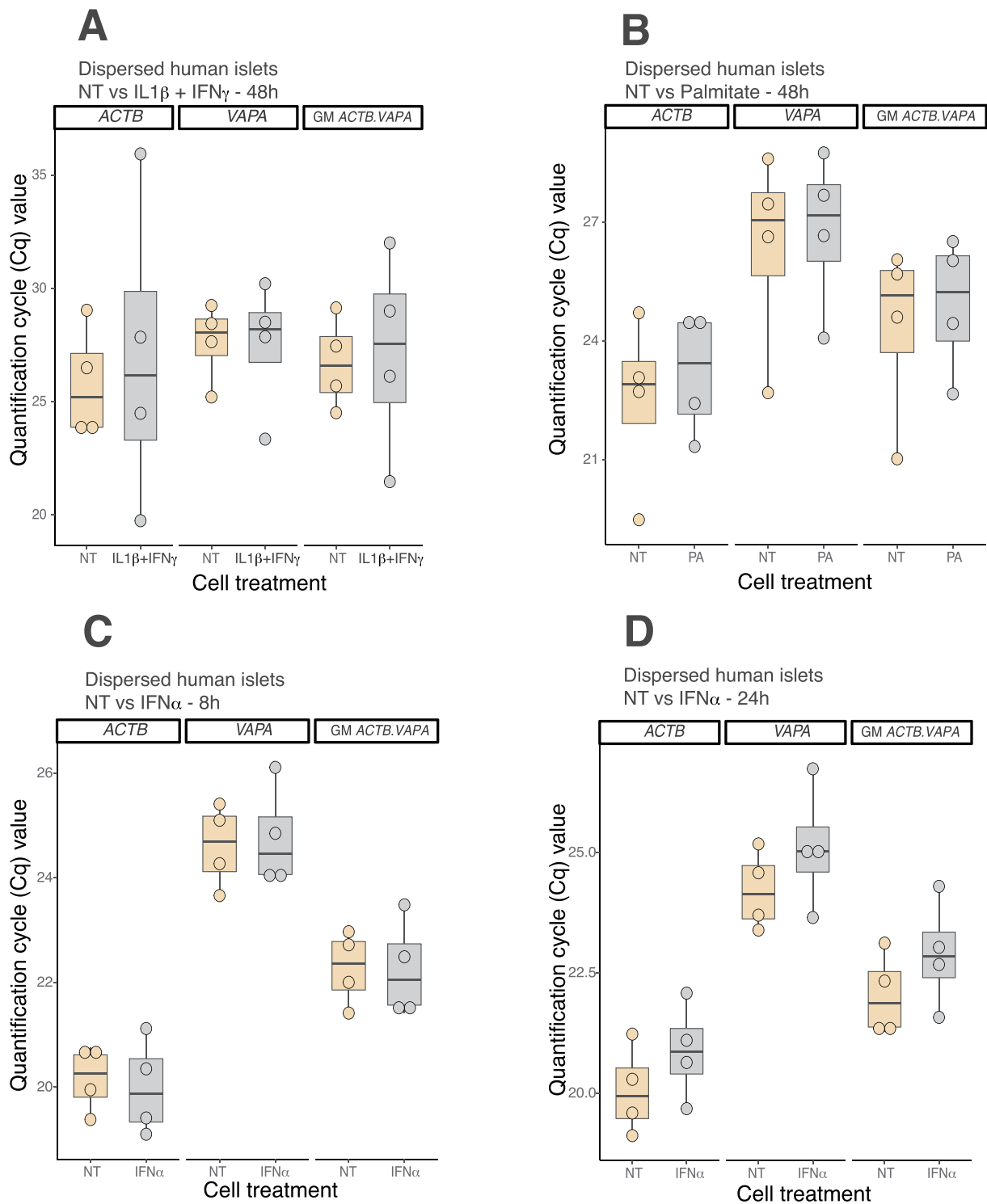


**Figure 3. Validation of reference genes by qPCR in dispersed human islet cells.** Distribution of the quantification cycle (Cq) value of five new and two commonly used reference genes (*ACTB* and *GAPDH*) based on qPCR, in human islet cells treated with IL1 $\beta$  + IFN $\gamma$  for 48 h (A), palmitate for 48 h (B), IFN $\alpha$  for 8 h (C) and 24 h (D). Geometric means of *ACTB* and *VAPA* Cq values were also calculated (GM *ACTB.VAPA*). The boxplots show the 25<sup>th</sup> and 75<sup>th</sup> percentiles, and the horizontal line represents the median. Each data point represents one qPCR replicate from four independent experiments. There is no statistical difference between the tested conditions (paired Student's t-test, condition versus not-treated (NT)).

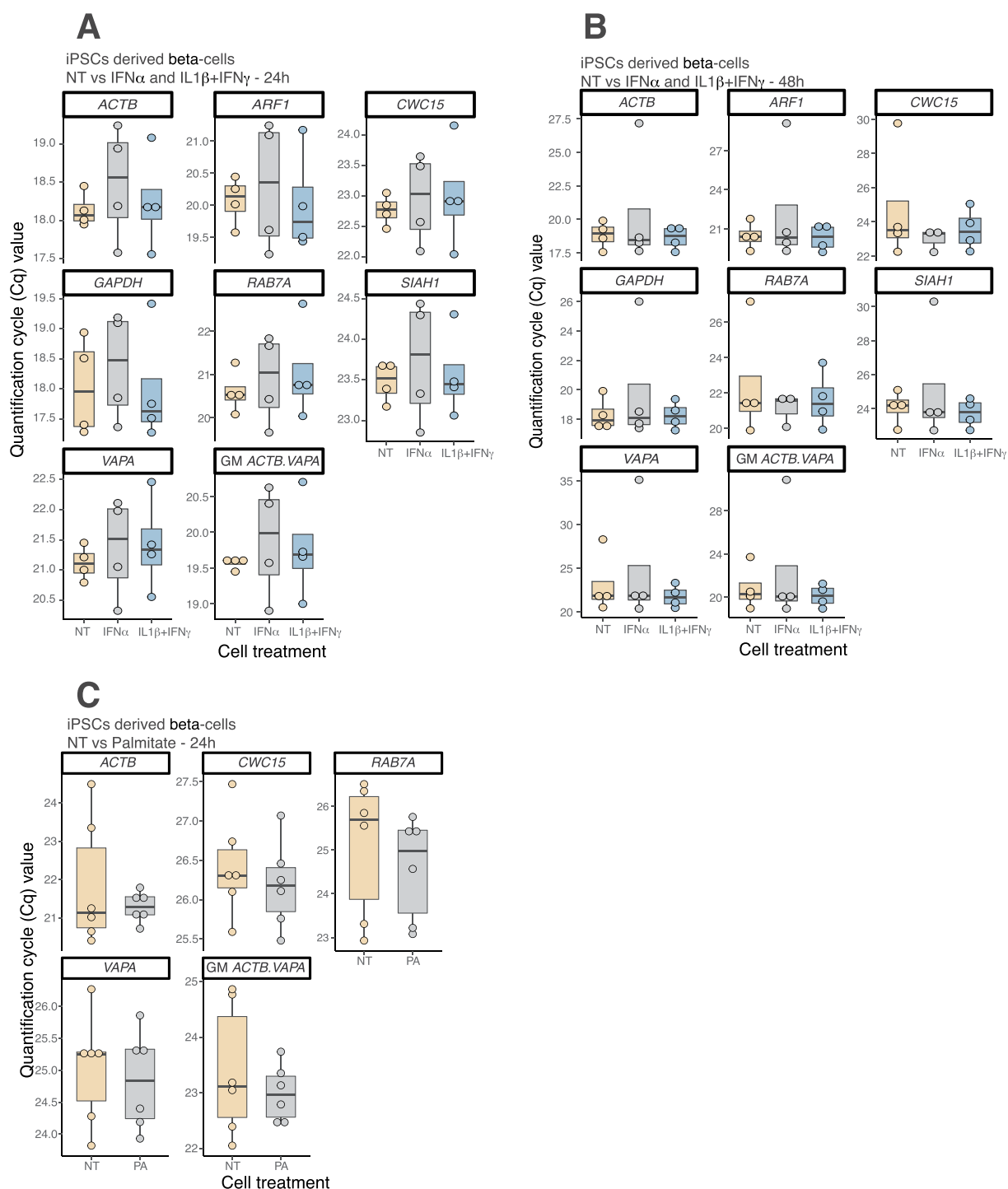


**Figure 4. Validation of reference genes by qPCR in human iPSC-derived beta cells.** Distribution of the quantification cycle (Cq) value of five new and two commonly used reference genes (*ACTB* and *GAPDH*) based on qPCR of human iPSC-derived beta cells treated with IL1 $\beta$  + IFN $\gamma$  and IFN $\alpha$  for 24 h (**A**), IL1 $\beta$  + IFN $\gamma$  and IFN $\alpha$  for 48 h (**B**), and the metabolic stressor palmitate for 24 h (**C**). Geometric means of *ACTB* and *VAPA* Cq values were also calculated (GM *ACTB.VAPA*). The human iPSC-derived beta cells treated with IL1 $\beta$  + IFN $\gamma$  and IFN $\alpha$  were derived from patients affected by Wolfram syndrome,<sup>23</sup> which should aggravate the endoplasmic reticulum stress. The human iPSC-derived beta cells treated with palmitate derived from control iPSC lines.<sup>24,25</sup> Each data point represents one qPCR replicate from four to six independent differentiations. The boxplots show the 25<sup>th</sup> and 75<sup>th</sup> percentiles, and the horizontal line represents the median. Results from four to six independent experiments. There is no statistical difference between the tested conditions (paired Student's t-test, condition versus not-treated (NT)). The scales are adjusted to each represented gene.

## Validation of the necessity for additional reference genes

To validate the normalization strategies for genes of particular interest in the context of islet inflammation, we compared mRNA expression of *IRF1* (a key transcription factor downstream of IFN $\alpha$  signaling in beta cells)<sup>22,33,34</sup> before and after *IRF1* knockdown in EndoC- $\beta$ H1 cells under basal conditions and following IFN $\alpha$  exposure. Normalization of *IRF1* expression by *ACTB* alone failed to show *IRF1* silencing following transfection with *IRF1* siRNA (Figure 5A). Normalization by *VAPA* alone failed to show *IRF1* silencing after transfection with the siRNA, but it revealed a significant decrease in *IRF1* expression after exposure to IFN $\alpha$  (Figure 5B). Normalization by the geometric mean of *ACTB* and *VAPA* unveiled a significant *IRF1* inhibition (Figure 5C), which is probably due to the reduced CV in all four conditions analyzed (Figure 5D).

Similarly, mRNA induction of *HLA-ABC* (a key component of islet antigen presentation in the context of T1D)<sup>35</sup> by IFN $\alpha$  (Figure 5E, F, G) was detected following normalization by the geometric mean of *VAPA* and *ACTB*, with several fold decreased CV (Figure 5H). Additionally, we used *ACTB*, *VAPA* or the geometric mean between *ACTB* and *VAPA* mRNA expression for the normalization of *SRSF6* expression (*SRSF6* is a key serine and arginine-rich (SR) splicing factor involved in beta cell function and survival)<sup>36</sup> and of c-Jun N-terminal kinase 1 (*JNK1*; a kinase that under stress conditions contribute to beta cell apoptosis) (Supplementary Figure 3). The normalization by *VAPA* (alone or as a geometric mean with *ACTB*) reduced the variability (lower coefficient of variation) (Supplementary Figure 3D) of the *SRSF6* expression values under the different tested conditions as compared to normalization by *ACTB* alone (Supplementary

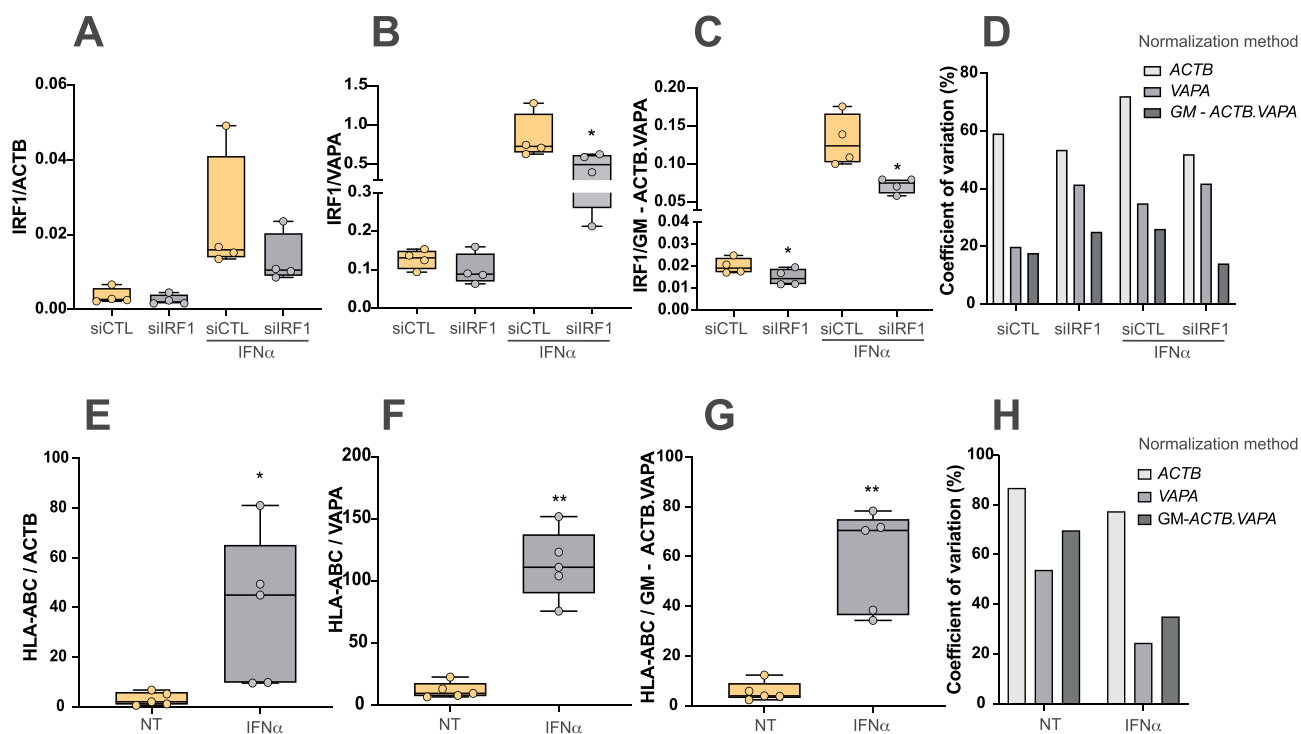


**Figure 5.** Quantification of *IRF1*, *HLA-ABC* mRNA expression in EndoC- $\beta$ H1 cells. EndoC- $\beta$ H1 cells were transfected with control siRNA (siCTL) or siRNA against *IRF1* (siIRF1), for 48 h, and then treated with IFN $\alpha$  for 24 h. *IRF1* mRNA expression was normalized to *ACTB* (A), *VAPA* (B) and to the geometric mean of *ACTB* and *VAPA* (C). Normalization by the geometric mean of *ACTB* and *VAPA* decreases *IRF1* expression variability (lower CV) (D). EndoC- $\beta$ H1 cells were treated with IFN $\alpha$  for 24 h and *HLA-ABC* expression was normalized to *ACTB* (E), *VAPA* (F) and to the geometric mean of *ACTB* and *VAPA* (G). Normalization by the geometric mean of *ACTB* and *VAPA* decreases *HLA-ABC* expression variability (lower CV) (H). The boxplots show the 25<sup>th</sup> and 75<sup>th</sup> percentiles, and the horizontal line represents the median. Each data point represents one qPCR replicate from four to five independent experiments. \*P < .05, \*\*P < .01 versus not-treated (NT) or siCTL (paired Student's t-test).



Figure 3A-D). Regarding *JNK1*, the normalization of gene expression after its KD using a specific siRNA was not affected by the normalization methods used (Supplementary Figure 3E, F, G, H), probably due to the high *JNK1* KD efficiency (>80%).

## Discussion

We presently combined different strategies to identify new reference genes for qPCR analysis in human pancreatic beta cells. We used RNA-seq data from beta cells or human islets exposed to different stresses and identified 264 top stably expressed genes. These genes are mostly related to cellular housekeeping functions, as indicated by the fact that they are enriched in GO biological pathways related to intracellular (protein) transport, mRNA metabolic processes etc. (Figure 1E). Following qPCR validation in independent samples, we found that the five candidate reference genes *ARF1*, *CWC15*, *RAB7A*, *SIAH1* and *VAPA* fit the criteria of 'suitable reference genes'.<sup>26</sup> These genes have stable transcript abundance under all biologic contexts tested and are, in general, comparable to the expression of target genes. Since the geometric mean of two or more reference genes provides a more accurate correction,<sup>17</sup> we selected *VAPA* and *ACTB* as a suitable compromise between a novel, highly stable mRNA, and a well-established but more variable reference mRNA.

Our data indicate that the geometric mean of *ACTB* and *VAPA* expression represents a valid normalization strategy, as these genes are stably expressed (present data) and their combined use reduces the CV of target genes such as *IRF1*, *HLA* class I, and *SRSF6* (Figure 5, Supplementary Figure 3A-D). The inclusion of *VAPA* as an additional normalization gene seems to be particularly important when the modification in terms of gene expression is subtle, such as a siRNA-induced inhibition of gene expression between 30% and 50%. qPCR guidelines suggest to use at least 3 reference genes,<sup>26</sup> but taking into account the scarcity of human islets, and the present data showing that it is possible to obtain reliable data using only two reference genes, we suggest that the geometric mean of *ACTB* and *VAPA* provides a fair compromise.

*ACTB* encodes one of six different actin isoforms, and has been widely used as a ubiquitously expressed reference gene.<sup>37</sup> Actin-B protein is highly conserved, and maintains cell structure, integrity, and motility.<sup>38,39</sup> Its rate of transcription is affected by mitogenic stimuli such as epidermal growth factor, transforming growth factor- $\beta$  (TGF- $\beta$ ) and platelet derived growth factor.<sup>40-42</sup> Since human beta cells proliferate very little,<sup>43</sup> this should not present a major issue when using *ACTB* as reference gene.

*VAPA* encodes a protein involved in the formation of endoplasmic reticulum contacts with other membranes, such as the Golgi complex and endosomes.<sup>44,45</sup> It participates in fundamental physiological processes such as vesicle trafficking, membrane fusion, protein complex assembly and cell motility.<sup>46,47</sup> The role of *VAPA* is consistent with housekeeping functions and its expression does not change under the presently tested experimental conditions. Of relevance, *VAPA* expression is not changed in beta cells from T1D patients or whole islets from T2D patients.

In conclusion, the present study identified a panel of genes that can be used as reference for qPCR studies in human beta cells (Supplementary Table 1). The geometric mean of two of these, namely *ACTB* and *VAPA*, may provide a robust normalization tool in the study of human beta cells. It will be important to confirm in different experimental conditions that neither *ACTB* nor *VAPA* is changed. Should this be the case, the other presently identified reference genes may be tested as an alternative approach.

## Material and methods

### Culture of human cells, gene silencing and treatments

The human beta cell line EndoC- $\beta$ H1 was provided by Dr R. Scharfmann (Institut Cochin, Université Paris Descartes, Paris, France).<sup>48</sup> EndoC- $\beta$ H1 cells were cultured in Dulbecco's Modified Eagle Medium (DMEM) containing 5.6 mmol/L glucose (Gibco, Thermo Fisher Scientific), 2% fatty acid-free bovine serum albumin (BSA) fraction V (Roche), 50  $\mu$ mol/L 2-mercaptoethanol (Sigma-Aldrich), 10 mmol/L nicotinamide (Calbiochem),

5.5 µg/mL transferrin (Sigma-Aldrich), 6.7 ng/mL selenite (Sigma-Aldrich), 100 U/mL penicillin + 100 µg/mL streptomycin (Lonza) in matrigel–fibronectin–coated plates.<sup>49</sup>

Human islets were isolated from non-diabetic organ donors by collagenase digestion and density gradient purification and characterized as previously reported.<sup>50</sup> (Supplementary Table 2), with the approval of the local Ethical Committee in Pisa, Italy. After isolation, the islets were cultured in M199 culture medium (5.5 mmol/L glucose) and shipped to our laboratory. On arrival, the islets were cultured in Ham's F-10 medium containing 6.1 mmol/L glucose (Gibco, Thermo-Fisher Scientific), 10% fetal bovine serum (Gibco, Thermo-Fisher Scientific), 2 mmol/L GlutaMAX (Sigma-Aldrich), 50 mmol/L 3-isobutyl-1-methylxanthine (Sigma-Aldrich), 1% fatty acid-free BSA fraction V, 50 U/mL penicillin and 50 mg/mL streptomycin.<sup>49</sup>

The iPSC lines HEL46.11,<sup>25</sup> and HEL115.6<sup>24</sup> were derived from human neonatal foreskin and umbilical cord fibroblasts, respectively. The iPSC line Wolf2010-9 was kindly provided by Dr. Fumihiko Urano (Washington University School of Medicine, St. Louis, MO, USA) and it is derived from patients with Wolfram syndrome.<sup>23</sup> iPSCs were cultured in E8 medium (Life Technologies) in matrigel-coated plates (Corning BV, Life Sciences). iPSCs were differentiated into pancreatic beta cells using a 7-step protocol as previously described.<sup>24,25,51,52</sup>

EndoC-βH1 cells, dispersed human islet cells and iPSC-beta cells were exposed to human pro-inflammatory cytokines IL1β (50 U/mL; R&D Systems) and IFNγ (1,000 U/mL; PeproTech) for 48 h and/or 24 h, as described.<sup>2,28</sup> EndoC-βH1 cells, dispersed pancreatic islets and iPSC-beta cells were exposed to human IFNα (2,000 U/mL; PeproTech) alone for 8 h/24 h, 8 h/24 h and 24 h/48 h, respectively.<sup>28,53,54</sup> EndoC-βH1 cells were also exposed to a combination of IL1β (50 U/mL; R&D Systems) and IFNα for 48 h.<sup>53,54</sup> These conditions are based on previously published time course and dose-response experiments.<sup>49,53</sup>

Dispersed human islets and iPSC-beta cells were exposed to 0.5 mmol/L palmitate (Sigma-Aldrich) for 48 h and 24 h, respectively.<sup>1,4,55</sup>

EndoC-βH1 cells were exposed to thapsigargin (1 µM; Millipore-Sigma) and tunicamycin (5 µg/

mL; Sigma-Aldrich) for 24 h and 48 h, respectively.<sup>56,57</sup> These conditions are summarized in Table 1.

## RNA-sequencing

The RNA-seq experiments of EndoC-βH1 cells, dispersed human islets, and islets from T2D patients were previously published by our group.<sup>22,50,58</sup> RNA-seq data of FACS-purified beta cells from T1D patients was downloaded via the Gene Expression Omnibus (GEO) repository.<sup>59</sup> All RNA-seq data were re-analyzed using our own and updated pipeline. Initial quality control of reads was assessed using FastQC (version 0.11.5; FastQC: A quality control tool for high throughput sequence data [Online]. Available at: <http://www.bioinformatics.babraham.ac.uk/projects/fastqc/>) and gene expression was quantified (in TPM) using Salmon v1.3.0,<sup>60</sup> with extra parameters “–seqBias –gcBias –validateMappings.” The reference genome (GENCODE gene annotation release 31)<sup>20</sup> was indexed using default parameters. Differentially expressed genes were assessed using DESeq2 version 1.28.1.<sup>61</sup> The Generalized Linear Model was fitted with the formula “design ~ pairing + condition” to account for the pair-wise experimental design (control and treatment) whenever possible. Genes were considered differently expressed if they passed a threshold of adjusted *P*-value <0.05 (Benjamini-Hochberg correction) and |fold-change| >1.5.

## Identification and selection of reference genes

From the DESeq2 analysis of RNA-seq datasets, genes not differentially expressed between paired conditions were selected. TPM values were used to evaluate intra – and inter – experimental variability by calculating the coefficient of variation (CV) of each gene for each group and condition. The CV is defined by the ratio of the standard deviation of a gene TPM to the arithmetic mean of the same gene. Next, we calculated the arithmetic mean of CV between different conditions. Genes with a mean CV <0.10 (10%) were selected for further analysis. TPM values from the different conditions were averaged and the mean CV was evaluated within three subgroups of expression, namely

genes with TPM between 10–100, 100–1000 and 1000–10000.

### Functional annotation

Functional enrichment was performed in R using clusterProfiler,<sup>62</sup> and enrichplot<sup>63</sup> packages for Gene Ontology. The genes identified by RNA-seq in EndoC- $\beta$ H1 cells and human islets with TPM >0.5 under control condition or after treatment were considered as expressed and used as background. An adjusted *P*-value <0.05 (Benjamini-Hochberg correction) was considered statistically significant.

### mRNA extraction, cDNA synthesis and quantification by qPCR

Poly(A)+ mRNA was isolated using Dynabeads mRNA Direct kit (Invitrogen), following the manufacturer's protocol. mRNA was reverse transcribed using the Reverse Transcriptase Core kit (Eurogentec). In order to reduce variability in mRNA input, cDNA was quantified using the NanoDrop spectrophotometer (NanoDrop ND-1000; Thermo Fisher Scientific). Samples were then diluted to the same concentration of the least-concentrated sample (EndoC- $\beta$ H1 cells were diluted to 800 ng/ $\mu$ L; dispersed human islets to 500 ng/ $\mu$ L; iPSC-beta cells to 300 ng/ $\mu$ L). Primers were designed using Primer-BLAST software,<sup>64</sup> using the following criteria: (I) primers were designed across exon-exon junction whenever possible; (II) PCR amplicon size of 80 – 120 base pairs to minimize unwanted effects on the amplification efficiency; (III) primer T<sub>m</sub> (melting temperature) was 56–60°C (with an annealing temperature of approximately 58°C); (IV) primer GC content was 40–65%, with no dimer or hairpin secondary structures. The qPCR amplification was done using IQ SYBR Green Supermix (Bio-Rad) using the CFX Connect Real-Time PCR Detection System (Bio-Rad). The amplification efficiency of each primer pair was evaluated using a standard curve,<sup>65</sup> generated from six dilutions of cDNA (10<sup>7</sup> to 10<sup>2</sup> mRNA copies per microliter (copies per  $\mu$ L)). The target gene concentration was expressed as copies per  $\mu$ L.<sup>65</sup> The C<sub>q</sub> values specify the number of amplification cycles needed to detect a signal. Because C<sub>q</sub>

values are inversely correlated with the amount of target nucleotides, they were used to evaluate gene expression and extrapolate gene expression variability.

The cycling conditions were 95°C from 3 minutes (min), followed by 40 cycles of 95°C for 15 seconds (sec), and 58°C for 20 sec, followed by a final step of 95°C for 1 min, 70°C for 5 sec, and 95°C for 50 sec. For each gene, the melting curve was analyzed to confirm amplification of a single PCR product. Primers are listed in **Supplementary Table 3**.

### Analysis of single-cell RNA-sequencing

Raw sequencing data was obtained from the Human Pancreas Analysis Program (HPAP).<sup>27</sup> The metadata related to the samples are summarized in **Supplementary Table 4**. All samples were aligned and the quality control accessed through 10X Genomics Cellranger v6.0.0<sup>66</sup> with the GRCh37 reference genome. The filtered expression matrices (from the “filtered\_feature\_bc\_matrix” output of Cellranger) from each sample were then imported and analyzed using Seurat v4.0.1.<sup>67</sup> Each sample was then individually inspected for the UMI (Unique Molecular Identifier) and the number of genes identified. In order to remove potentially empty droplets and/or low-quality cells that could bias the analysis, the cells were selected based on the percentage of mitochondrial gene content (<10%), number of genes detected (>1000), and UMI (>3000-3500). The expression matrices were merged, and the data were normalized to uniform read depth for each cell, log-transformed, regressed out to the percentage of mitochondrial genes and integrated with the Harmony algorithm<sup>68</sup> using the top 50 Principal Components (PC) of the PCA. The sample identifier and the donors' gender were used as confounding factors. The number of iteration was set at a maximum of 20 (max.iter.harmony = 20) and the lambda for the ridge regression penalty parameter was set at 0.5 and 1 for non-diabetic donors' samples (ND) for sample identifier and the donors' gender confounding factors, respectively. The default parameters were used for the analysis of the T1D dataset. Both analyses converged before the maximum of number of iterations was reached (12 for ND, 6 for T1D). The first 50 PC generated by Harmony were used to

compute the Shared Nearest Neighbor (SNN) ( $k = 30$ ). Ultimately, the unsupervised clustering algorithm of Leiden<sup>69</sup> was used in order to reveal cell identities (resolution = 0.5).

The UMAP projections (Supplementary Figure 2A, B) were obtained using the first 50 PC obtained through Harmony analysis (min. dist = 0.3). The markers observed in each cluster were cross-validated by comparison with previously described markers.<sup>70</sup>

## Statistical analysis

Significant differences between experimental conditions were determined by Student's paired t-test or by ANOVA followed by Bonferroni correction as indicated.  $P$ -values  $< 0.05$  were considered statistically significant. Statistical tools used for RNA-seq analysis are described above. Violin plots illustrate kernel probability density (i.e., the width of the shaded area represents the data's density plot). The horizontal line represents the median, boxes quartiles, whiskers most extreme data values, and each data point represents one replicate of an independent experiment using islets from a different human donor, or an independent iPSC differentiation or an independent EndoC- $\beta$ H1 cell passage.

## Acknowledgments

The authors are grateful to Isabelle Millard, Anyishai Musuaya, Nathalie Pachera, Cai Ying, and Manon Depessemier (ULB Center for Diabetes Research) for providing excellent technical support.

## Disclosure statement

No potential conflict of interest was reported by the author(s).

## Funding

D.L.E. is funded by Welbio/FRFS (n° WELBIO-CR-2019C-04), Belgium, by the Dutch Diabetes Research Foundation (project Innovate2CureType1, DDRF; no. 2018.10.002) and by start-up funds provided by the Indiana Biosciences Research Institute; D.L.E. and M.C. are funded by the Brussels Region (INNOVIRIS BRIDGE grant DiaType); DLE, MC and PM are supported by the Innovative Medicines Initiative 2 Joint Undertaking under grant agreement 115797 (INNODIA) and 945268 (INNODIA

HARVEST). This Joint Undertaking receives support from the Union's Horizon 2020 research and innovation programme and the European Federation of Pharmaceutical Industries and Associations, JDRF, and The Leona M. and Harry B. Helmsley Charitable Trust; M.C. is funded by the Fonds National de la Recherche Scientifique and the Walloon Region SPW-EERWin2Wal project BetaSource, Belgium.

## Data accessibility

All raw RNA-sequencing data are accessible via NCBI Gene Expression Omnibus (GEO), access numbers GSE133218, GSE148058, GSE121863, GSE53949 and GSE159984. All raw scRNA-sequencing data are accessible via the HPAP portable (<https://hpap.pmacs.upenn.edu/>).

## References

1. Lytrivi M, Ghaddar K, Lopes M, Rosengren V, Piron A, Yi X, Johansson H, Lehtio J, Igoillo-Esteve M, Cunha DA, et al. Combined transcriptome and proteome profiling of the pancreatic beta-cell response to palmitate unveils key pathways of beta-cell lipotoxicity. *BMC Genomics*. 2020;21(1):590. doi:10.1186/s12864-020-07003-0.
2. Eizirik DL, Sammeth M, Bouckenooghe T, Bottu G, Sisino G, Igoillo-Esteve M, Ortis F, Santin I, Colli ML, Barthson J, et al. The human pancreatic islet transcriptome: expression of candidate genes for type 1 diabetes and the impact of pro-inflammatory cytokines. *PLoS Genet*. 2012;8(3):e1002552. doi:10.1371/journal.pgen.1002552.
3. Eizirik DL, Pasquali L, Cnop M. Pancreatic beta-cells in type 1 and type 2 diabetes mellitus: Different pathways to failure. *Nat Rev Endocrinol*. 2020;16(7):349–362. doi:10.1038/s41574-020-0355-7.
4. Cnop M, Abdulkarim B, Bottu G, Cunha DA, Igoillo-Esteve M, Masini M, Turatsinze JV, Griebel T, Villate O, Santin I, et al. Rna sequencing identifies dysregulation of the human pancreatic islet transcriptome by the saturated fatty acid palmitate. *Diabetes*. 2014;63(6):1978–1993. doi:10.2337/db13-1383.
5. VanGuilder HD, Vrana KE, Freeman WM. Twenty-five years of quantitative pcr for gene expression analysis. *Biotechniques*. 2008;44(5):619–626. doi:10.2144/000112776.
6. de Kok JB, Roelofs RW, Giesendorf BA, Pennings JL, Waas ET, Feuth T, Swinkels DW, Span PN. Normalization of gene expression measurements in tumor tissues: comparison of 13 endogenous control genes. *Lab Invest*. 2005;85(1):154–159. doi:10.1038/labinvest.3700208.
7. Lee PD, Sladek R, Greenwood CM, Hudson TJ. Control genes and variability: absence of ubiquitous reference

- transcripts in diverse mammalian expression studies. *Genome Res.* 2002;12(2):292–297. doi:10.1101/gr.217802.
8. Jo J, Choi S, Oh J, Lee SG, Choi SY, Kim KK, Park C. Conventionally used reference genes are not outstanding for normalization of gene expression in human cancer research. *BMC Bioinform.* 2019;20(Suppl 10):245. doi:10.1186/s12859-019-2809-2.
  9. Sharan RN, Vaiphei ST, Nongrum S, Keppen J, Ksoo M. Consensus reference gene(s) for gene expression studies in human cancers: End of the tunnel visible? *Cell Oncol (Dordr).* 2015;38(6):419–431. doi:10.1007/s13402-015-0244-6.
  10. Barber RD, Harmer DW, Coleman RA, Clark BJ. Gapdh as a housekeeping gene: Analysis of gapdh mrna expression in a panel of 72 human tissues. *Physiol Genomics.* 2005;21(3):389–395. doi:10.1152/physiolgenomics.00025.2005.
  11. Derks NM, Muller M, Gaszner B, Tilburg-Ouwens DT, Roubos EW, Kozicz LT. Housekeeping genes revisited: Different expressions depending on gender, brain area and stressor. *Neuroscience.* 2008;156(2):305–309. doi:10.1016/j.neuroscience.2008.07.047.
  12. Rodriguez-Mulero S, Montanya E. Selection of a suitable internal control gene for expression studies in pancreatic islet grafts. *Transplantation.* 2005;80(5):650–652. doi:10.1097/01.tp.0000173790.12227.7b.
  13. Kosinová L, Cahová M, Fabryová E, Tycová I, Koblas T, Leontovych I, Saudek F, Križ J. Unstable expression of commonly used reference genes in rat pancreatic islets early after isolation affects results of gene expression studies. *PLoS One.* 2016;11(4):e0152664. doi:10.1371/journal.pone.0152664.
  14. Moore F, Colli ML, Cnop M, Esteve MI, Cardozo AK, Cunha DA, Bugliani M, Marchetti P, Eizirik DL. Ptpn2, a candidate gene for type 1 diabetes, modulates interferon-gamma-induced pancreatic beta-cell apoptosis. *Diabetes.* 2009;58(6):1283–1291. doi:10.2337/db08-1510.
  15. Smidt K, Wogensen L, Brock B, Schmitz O, Rungby J. Real-time pcr: housekeeping genes in the ins-1e beta-cell line. *Horm Metab Res.* 2006;38(1):8–11. doi:10.1055/s-2006-924968.
  16. Pfaffl MW, Tichopad A, Prgomet C, Neuvians TP. Determination of stable housekeeping genes, differentially regulated target genes and sample integrity: bestkeeper--excel-based tool using pair-wise correlations. *Biotechnol Lett.* 2004;26(6):509–515. doi:10.1023/B:BILE.0000019559.84305.47.
  17. Vandesompele J, De Preter K, Pattyn F, Poppe B, Van Roy N, De Paepe A, Speleman F. Accurate normalization of real-time quantitative rt-pcr data by geometric averaging of multiple internal control genes. *Genome Biol.* 2002;3(7):RESEARCH0034. doi:10.1186/gb-2002-3-7-research0034.
  18. Andersen CL, Jensen JL, Orntoft TF. Normalization of real-time quantitative reverse transcription-pcr data: a model-based variance estimation approach to identify genes suited for normalization, applied to bladder and colon cancer data sets. *Cancer Res.* 2004;64(15):5245–5250. doi:10.1158/0008-5472.CAN-04-0496.
  19. Akilesh S, Shaffer DJ, Roopenian D. Customized molecular phenotyping by quantitative gene expression and pattern recognition analysis. *Genome Res.* 2003;13(7):1719–1727. doi:10.1101/gr.533003.
  20. Frankish A, Diekhans M, Ferreira AM, Johnson R, Jungreis I, Loveland J, Mudge JM, Sisu C, Wright J, Armstrong J, et al. Gencode reference annotation for the human and mouse genomes. *Nucleic Acids Res.* 2019;47(D1):D766–D773. doi:10.1093/nar/gky955.
  21. Eisenberg E, Levanon EY. Human housekeeping genes, revisited. *Trends Genet.* 2013;29(10):569–574. doi:10.1016/j.tig.2013.05.010.
  22. Colli ML, Ramos-Rodriguez M, Nakayasu ES, Alvelos MI, Lopes M, Hill JLE, Turatsinze JV, Coomans de Brachene A, Russell MA, Raurell-Vila H, et al. An integrated multi-omics approach identifies the landscape of interferon-alpha-mediated responses of human pancreatic beta cells. *Nat Commun.* 2020;11(1):2584. doi:10.1038/s41467-020-16327-0.
  23. Lu S, Kanekura K, Hara T, Mahadevan J, Spears LD, Osowski CM, Martinez R, Yamazaki-Inoue M, Toyoda M, Neilson A, et al. A calcium-dependent protease as a potential therapeutic target for wolfram syndrome. *Proc Natl Acad Sci U S A.* 2014;111(49):E5292–5301. doi:10.1073/pnas.1421055111.
  24. Cosentino C, Toivonen S, Diaz Villamil E, Atta M, Ravanat JL, Demine S, Schiavo AA, Pachera N, Deglasse JP, Jonas JC, et al. Pancreatic beta-cell trna hypomethylation and fragmentation link trmt10a deficiency with diabetes. *Nucleic Acids Res.* 2018;46(19):10302–10318. doi:10.1093/nar/gky839.
  25. Saarimäki-Vire J, Balboa D, Russell MA, Saarikettu J, Kinnunen M, Keskitalo S, Malhi A, Valensisi C, Andrus C, Eurola S, et al. An activating stat3 mutation causes neonatal diabetes through premature induction of pancreatic differentiation. *Cell Rep.* 2017;19(2):281–294. doi:10.1016/j.celrep.2017.03.055.
  26. Bustin SA, Benes V, Garson JA, Hellemans J, Huggett J, Kubista M, Mueller R, Nolan T, Pfaffl MW, Shipley GL, et al. The miqe guidelines: Minimum information for publication of quantitative real-time pcr experiments. *Clin Chem.* 2009;55(4):611–622. doi:10.1373/clinchem.2008.112797.
  27. Kaestner KH, Powers AC, Naji A, Consortium H, Atkinson MA. Nih initiative to improve understanding of the pancreas, islet, and autoimmunity in type 1 diabetes: The human pancreas analysis program (hpap). *Diabetes.* 2019;68(7):1394–1402. doi:10.2337/db19-0058.
  28. Demine S, Schiavo AA, Marin-Canas S, Marchetti P, Cnop M, Eizirik DL. Pro-inflammatory cytokines induce cell death, inflammatory responses, and endoplasmic reticulum stress in human ipsc-derived beta cells. *Stem Cell Res Ther.* 2020;11(1):7. doi:10.1186/s13287-019-1523-3.

29. De Franco E, Lytrivi M, Ibrahim H, Montaser H, Wakeling MN, Fantuzzi F, Patel K, Demarez C, Cai Y, Igoillo-Esteve M, et al. Yipf5 mutations cause neonatal diabetes and microcephaly through endoplasmic reticulum stress. *J Clin Invest.* 2020;130(12):6338–6353. doi:10.1172/JCI141455.
30. Lytrivi M, Senee V, Salpea P, Fantuzzi F, Philippi A, Abdulkarim B, Sawatani T, Marin-Canas S, Pachera N, Degavre A, et al. Dnajc3 deficiency induces beta-cell mitochondrial apoptosis and causes syndromic young-onset diabetes. *Eur J Endocrinol.* 2021;184(3):459–472. doi:10.1530/EJE-20-0636.
31. Leite NC, Sintov E, Meer TB, Brehm MA, Greiner DL, Harlan DM, Melton DA. Modeling type 1 diabetes in vitro using human pluripotent stem cells. *Cell Rep.* 2020;32(2):107894. doi:10.1016/j.celrep.2020.107894.
32. Ellis C, Ramzy A, Kieffer TJ. Regenerative medicine and cell-based approaches to restore pancreatic function. *Nat Rev Gastroenterol Hepatol.* 2017;14:612–628.
33. Moore F, Naamane N, Colli ML, Bouckennooghe T, Ortis F, Gurzov EN, Igoillo-Esteve M, Mathieu C, Bontempi G, Thykjaer T, et al. Stat1 is a master regulator of pancreatic beta-cell apoptosis and islet inflammation. *J Biol Chem.* 2011;286(2):929–941. doi:10.1074/jbc.M110.162131.
34. Colli ML, Hill JLE, Marroqui L, Chaffey J, Dos Santos RS, Leete P, Coomans de Brachene A, Paula FMM, Op de Beeck A, Castela A, et al. Pdl1 is expressed in the islets of people with type 1 diabetes and is up-regulated by interferons-alpha and-gamma via irf1 induction. *EBioMedicine.* 2018;36:367–375. doi:10.1016/j.ebiom.2018.09.040.
35. Richardson SJ, Rodriguez-Calvo T, Gerling IC, Mathews CE, Kaddis JS, Russell MA, Zeissler M, Leete P, Krogvold L, Dahl-Jorgensen K, et al. Islet cell hyperexpression of hla class i antigens: a defining feature in type 1 diabetes. *Diabetologia.* 2016;59(11):2448–2458. doi:10.1007/s00125-016-4067-4.
36. Juan-Mateu J, Alvelos MI, Turatsinze JV, Villate O, Lizarraga-Mollinedo E, Grieco FA, Marroqui L, Bugliani M, Marchetti P, Eizirik DL. Srp55 regulates a splicing network that controls human pancreatic beta-cell function and survival. *Diabetes.* 2018;67(3):423–436. doi:10.2337/db17-0736.
37. Rubenstein PA. The functional importance of multiple actin isoforms. *Bioessays.* 1990;12(7):309–315. doi:10.1002/bies.950120702.
38. Pollard TD, Borisy GG. Cellular motility driven by assembly and disassembly of actin filaments. *Cell.* 2003;112(4):453–465. doi:10.1016/S0092-8674(03)00120-X.
39. Bunnell TM, Burbach BJ, Shimizu Y, Ervasti JM. Beta-actin specifically controls cell growth, migration, and the g-actin pool. *Mol Biol Cell.* 2011;22(21):4047–4058. doi:10.1091/mbc.e11-06-0582.
40. Leof EB, Proper JA, Getz MJ, Moses HL. Transforming growth factor type beta regulation of actin mRNA. *J Cell Physiol.* 1986;127(1):83–88. doi:10.1002/jcp.1041270111.
41. Keski-Oja J, Raghov R, Sawdey M, Loskutoff DJ, Postlethwaite AE, Kang AH, Moses HL. Regulation of mRNAs for type-1 plasminogen activator inhibitor, fibronectin, and type I procollagen by transforming growth factor-beta. Divergent responses in lung fibroblasts and carcinoma cells. *J Biol Chem.* 1988;263(7):3111–3115. doi:10.1016/S0021-9258(18)69042-8.
42. Elder PK, Schmidt LJ, Ono T, Getz MJ. Specific stimulation of actin gene transcription by epidermal growth factor and cycloheximide. *Proc Natl Acad Sci U S A.* 1984;81(23):7476–7480. doi:10.1073/pnas.81.23.7476.
43. Cnop M, Hughes SJ, Igoillo-Esteve M, Hoppa MB, Syyed F, van de Laar L, Gunter JH, de Koning EJ, Walls GV, Gray DW, et al. The long lifespan and low turnover of human islet beta cells estimated by mathematical modelling of lipofuscin accumulation. *Diabetologia.* 2010;53(2):321–330. doi:10.1007/s00125-009-1562-x.
44. Alpy F, Rousseau A, Schwab Y, Legueux F, Stoll I, Wendling C, Spiegelhalter C, Kessler P, Mathelin C, Rio MC, et al. Stard3 or stard3nl and vap form a novel molecular tether between late endosomes and the ER. *J Cell Sci.* 2013;126(Pt 23):5500–5512. doi:10.1242/jcs.139295.
45. Peretti D, Dahan N, Shimoni E, Hirschberg K, Lev S. Coordinated lipid transfer between the endoplasmic reticulum and the golgi complex requires the vap proteins and is essential for golgi-mediated transport. *Mol Biol Cell.* 2008;19(9):3871–3884. doi:10.1091/mbc.e08-05-0498.
46. Phillips MJ, Voeltz GK. Structure and function of ER membrane contact sites with other organelles. *Nat Rev Mol Cell Biol.* 2016;17(2):69–82. doi:10.1038/nrm.2015.8.
47. Prinz WA. Bridging the gap: Membrane contact sites in signaling, metabolism, and organelle dynamics. *J Cell Biol.* 2014;205(6):759–769. doi:10.1083/jcb.201401126.
48. Ravassard P, Hazhouz Y, Pechberty S, Bricout-Neveu E, Armanet M, Czernichow P, Scharfmann R. A genetically engineered human pancreatic beta cell line exhibiting glucose-inducible insulin secretion. *J Clin Invest.* 2011;121(9):3589–3597. doi:10.1172/JCI58447.
49. Brozzi F, Nardelli TR, Lopes M, Millard I, Barthson J, Igoillo-Esteve M, Grieco FA, Villate O, Oliveira JM, Casimir M, et al. Cytokines induce endoplasmic reticulum stress in human, rat and mouse beta cells via different mechanisms. *Diabetologia.* 2015;58(10):2307–2316. doi:10.1007/s00125-015-3669-6.
50. Marselli L, Piron A, Suleiman M, Colli ML, Yi X, Khamis A, Carrat GR, Rutter GA, Bugliani M, Giusti L, et al. Persistent or transient human beta cell dysfunction induced by metabolic stress: specific signatures and shared gene expression with type 2 diabetes. *Cell Rep.* 2020;33(9):108466.
51. Pagliuca FW, Millman JR, Gurtler M, Segel M, Van Dervort A, Ryu JH, Peterson QP, Greiner D, Melton DA. Generation of functional human pancreatic beta cells in vitro. *Cell.* 2014;159:428–439.

52. Rezania A, Bruin JE, Arora P, Rubin A, Batushansky I, Asadi A, O'Dwyer S, Quiskamp N, Mojibian M, Albrecht T, et al. Reversal of diabetes with insulin-producing cells derived in vitro from human pluripotent stem cells. *Nat Biotechnol.* 2014;32(11):1121–1133. doi:10.1038/nbt.3033.
53. Marroqui L, Dos Santos RS, Op de Beeck A, Coomans de Brachene A, Marselli L, Marchetti P, Eizirik DL. Interferon-alpha mediates human beta cell hla class i overexpression, endoplasmic reticulum stress and apoptosis, three hallmarks of early human type 1 diabetes. *Diabetologia.* 2017;60(4):656–667. doi:10.1007/s00125-016-4201-3.
54. Coomans de Brachene A, Castela A, Op de Beeck A, Mirmira RG, Marselli L, Marchetti P, Masse C, Miao W, Leit S, Evans-Molina C, et al. Preclinical evaluation of tyrosine kinase 2 inhibitors for human beta-cell protection in type 1 diabetes. *Diabetes Obes Metab.* 2020;22(10):1827–1836. doi:10.1111/dom.14104.
55. Bugliani M, Masini M, Liechti R, Marselli L, Xenarios I, Boggi U, Filipponi F, Masiello P, Marchetti P. The direct effects of tacrolimus and cyclosporin a on isolated human islets: a functional, survival and gene expression study. *Islets.* 2009;1(2):106–110. doi:10.4161/isl.1.2.9142.
56. Paula FMM, Leite NC, Borck PC, Freitas-Dias R, Cnop M, Chacon-Mikahil MPT, Cavaglieri CR, Marchetti P, Boschero AC, Zoppi CC, et al. Exercise training protects human and rodent beta cells against endoplasmic reticulum stress and apoptosis. *FASEB J.* 2018;32(3):1524–1536. doi:10.1096/fj.201700710R.
57. Tsonkova VG, Sand FW, Wolf XA, Grunnet LG, Kirstine Ringgaard A, Ingvorsen C, Winkel L, Kalisz M, Dalgaard K, Bruun C, et al. The endoc-betah1 cell line is a valid model of human beta cells and applicable for screenings to identify novel drug target candidates. *Mol Metab.* 2018;8:144–157. doi:10.1016/j.molmet.2017.12.007.
58. Ramos-Rodríguez M, Raurell-Vila H, Colli ML, Alvelos MI, Subirana-Granés M, Juan-Mateu J, Norris R, Turatsinze JV, Nakayasu ES, Webb-Robertson BM, et al. The impact of proinflammatory cytokines on the beta-cell regulatory landscape provides insights into the genetics of type 1 diabetes. *Nat Genet.* 2019;51(11):1588–1595.
59. Russell MA, Redick SD, Blodgett DM, Richardson SJ, Leete P, Krogvold L, Dahl-Jorgensen K, Bottino R, Brissova M, Spaeth JM, et al. Hla class ii antigen processing and presentation pathway components demonstrated by transcriptome and protein analyses of islet beta-cells from donors with type 1 diabetes. *Diabetes.* 2019;68(5):988–1001. doi:10.2337/db18-0686.
60. Patro R, Duggal G, Love MI, Irizarry RA, Kingsford C. Salmon provides fast and bias-aware quantification of transcript expression. *Nat Methods.* 2017;14(4):417–419. doi:10.1038/nmeth.4197.
61. Love MI, Huber W, Anders S. Moderated estimation of fold change and dispersion for rna-seq data with deseq2. *Genome Biol.* 2014;15(12):550. doi:10.1186/s13059-014-0550-8.
62. Yu G, Wang LG, Han Y, He QY. Clusterprofiler: An r package for comparing biological themes among gene clusters. *OMICS.* 2012;16(5):284–287. doi:10.1089/omi.2011.0118.
63. Yu G. Enrichplot: visualization of functional enrichment result. *R Package Version.* 2020;1:8.1.
64. Ye J, Coulouris G, Zaretskaya I, Cutcutache I, Rozen S, Madden TL. Primer-blast: a tool to design target-specific primers for polymerase chain reaction. *BMC Bioinform.* 2012;13(1):134. doi:10.1186/1471-2105-13-134.
65. Overbergh L, Valckx D, Waer M, Mathieu C. Quantification of murine cytokine mrnas using real time quantitative reverse transcriptase pcr. *Cytokine.* 1999;11(4):305–312. doi:10.1006/cyto.1998.0426.
66. Zheng GX, Terry JM, Belgrader P, Ryvkin P, Bent ZW, Wilson R, Ziraldo SB, Wheeler TD, McDermott GP, Zhu J, et al. Massively parallel digital transcriptional profiling of single cells. *Nat Commun.* 2017;8(1):14049. doi:10.1038/ncomms14049.
67. Stuart T, Butler A, Hoffman P, Hafemeister C, Papalexi E, Mauck WM 3rd, Hao Y, Stoekius M, Smibert P, Satija R. Comprehensive integration of single-cell data. *Cell.* 2019;177(7):1888–1902 e1821. doi:10.1016/j.cell.2019.05.031.
68. Korsunsky I, Millard N, Fan J, Slowikowski K, Zhang F, Wei K, Baglaenko Y, Brenner M, Loh PR, Raychaudhuri S. Fast, sensitive and accurate integration of single-cell data with harmony. *Nat Methods.* 2019;16:1289–1296.
69. Traag VA, Waltman L, Van Eck NJ. From louvain to leiden: guaranteeing well-connected communities. *Sci Rep.* 2019;9(1):5233. doi:10.1038/s41598-019-41695-z.
70. Bosi E, Marselli L, De Luca C, Suleiman M, Tesi M, Ibberson M, Eizirik DL, Cnop M, Marchetti P. Integration of single-cell datasets reveals novel transcriptomic signatures of beta-cells in human type 2 diabetes. *NAR Genom Bioinform.* 2020;2(4):lqaa097. doi:10.1093/nargab/lqaa097.